IMMUNOLOGY

Direct measurement of T cell receptor affinity and sequence from naïve antiviral T cells

Shu-Qi Zhang,[1] Patricia Parker,[2] Ke-Yue Ma,[3] Chenfeng He,[2] Qian Shi,[2]* Zhonghao Cui,[2] Chad M. Williams,[2] Ben S. Wendel,[1] Amanda I. Meriwether,[2] Mary Alice Salazar,[2] Ning Jiang[2,3]†

T cells recognize and kill a myriad of pathogen-infected or cancer cells using a diverse set of T cell receptors (TCRs). The affinity of TCR to cognate antigen is of high interest in adoptive T cell transfer immunotherapy and antigen-specific T cell repertoire immune profiling because it is widely known to correlate with downstream T cell responses. We introduce the in situ TCR affinity and sequence test (iTAST) for simultaneous measurement of TCR affinity and sequence from single primary CD8$^+$ T cells in human blood. We demonstrate that the repertoire of primary antigen-specific T cells from pathogen-inexperienced individuals has a surprisingly broad affinity range of 1000-fold composed of diverse TCR sequences. Within this range, samples from older individuals contained a reduced frequency of high-affinity T cells compared to young individuals, demonstrating an age-related effect of T cell attrition that could cause holes in the repertoire. iTAST should enable the rapid selection of high-affinity TCRs ex vivo for adoptive immunotherapy and measurement of T cell response for immune monitoring applications.

INTRODUCTION

CD8$^+$ T lymphocytes are a subclass of T cells that directly kills cancer and pathogen-infected cells through recognition of peptide bound to major histocompatibility complex (pMHC) using its T cell receptor (TCR) (*1*). The affinity of a TCR to a given peptide epitope is dependent on its TCR sequence, which affects the downstream fate (*2*) and functional capacity (*3*) of T cells by modulating TCR signaling strength (*4*) and proliferation rates (*3*, *5*). TCR-pMHC affinity is widely known to be a major determinant in the efficacy of adoptive T cell transfer (ACT) therapy. Thus, the ability to track TCR-pMHC affinity of single antigen-specific T cells within humans can provide important information on the quality of an immune response and for selecting the optimum T cells for ACT immunotherapy in cancer (*6*) and persistent viral infections (*7*, *8*).

Measurement of TCR properties is inherently difficult because each T cell contains its own unique TCR that can recognize a distinct set of pMHC ligands. The "gold standard" for measuring TCR-pMHC affinity is surface plasmon resonance (SPR), which requires the production of recombinant soluble TCR. The polyclonal nature of T cells makes SPR measurement extremely laborious and low throughput.

Several methods to measure TCR-pMHC kinetics and affinity from live T cells have recently been developed. Fluorescence microscopy–based assays can measure the TCR-pMHC dissociation rate of soluble pMHCs bound to the T cell (*7*). TCR-pMHC two-dimensional (2D) kinetics and affinity have also been measured in this manner using a fluorescence resonance energy transfer system (*9*). The throughput of these methods is limited by the field of view. In addition, more than 10^4 antigen-specific T cells must be added to the chamber to measure the kinetics of ~50 cells, which is not usually obtainable in a single human blood draw (*7*). The micropipette adhesion frequency assay is another method that can measure 2D TCR-pMHC kinetics and affinity but without requirements on cell input count (*5*). However, this assay is not suited to measure 2D affinities on primary T cells because the frequency of antigen-specific T cells are very low, especially precursor cells in antigen-inexperienced individuals, and there is a high degree of inefficiency due to time spent on nonreactive T cells. This has limited its use to either mouse models of infection (*10*), T cell clones, or TCR transgenic mouse systems (*5*, *11*). In vitro T cell expansion into a monoclonal population has its own disadvantages; besides the time and labor associated with in vitro expansion, the resulting T cell clones might not represent the starting primary T cell population because each T cell has a different proliferative potential (*12*). In addition, none of these methods can easily link TCR-pMHC binding parameters to TCR sequence, which provides information on T cell clonal expansion and lineage (*13*).

Here, we introduce in situ TCR affinity and sequence test (iTAST) that enables measurement of single-cell 2D TCR affinity and sequence directly from primary CD8$^+$ T cells obtained from single human blood draws, at a throughput of up to ~75 cells per day. We show that iTAST provides an accurate assessment of TCR affinity at the single-cell level that strongly correlates with TCR affinity by SPR, conventional 2D affinity (*5*), and cell functional capacity. We applied iTAST to study the naïve repertoire of hepatitis C virus (HCV)–specific CD8$^+$ T cells within healthy individuals and discovered a wide TCR affinity range that is dependent on age. The ability to obtain correlated TCR affinity and sequence information generated by iTAST should enable the rapid selection of high-affinity TCRs for adoptive immunotherapy.

RESULTS

Overview of iTAST

iTAST uses streptamers (*14*), which are pMHC multimers that can reversibly label antigen-specific CD8$^+$ T cells, the micropipette adhesion assay (*5*, *11*, *15*) for measurement of conventional 2D TCR affinity, and single-cell TCR sequencing (*13*). Low-frequency antigen-specific CD8$^+$ T cells are first isolated with streptamers using magnetic enrichment (*16*) and fluorescence-activated cell sorting (Fig. 1, A and B). Streptamers are then dissociated off of T cells using an excess amount of biotin, freeing their TCRs for interrogation with pMHC-coated red blood cells (RBCs) for single-cell 2D affinity measurement. After affinity testing, each cell is picked into a polymerase chain reaction (PCR) tube with a transfer micropipette

[1]McKetta Department of Chemical Engineering, University of Texas at Austin, Austin, TX 78712, USA. [2]Department of Biomedical Engineering, University of Texas at Austin, Austin, TX 78712, USA. [3]Institute for Cell and Molecular Biology, University of Texas at Austin, Austin, TX 78712, USA.
*Present address: Shanghai Jiao Tong University, Shanghai 200240, China.
†Corresponding author. Email: jiang@austin.utexas.edu

for TCR sequencing (Fig. 1C). Both TCR α and β chains are amplified by nested PCR with a molecular barcode imbedded for each tube, which is later used for α and β chain pairing (Fig. 1D).

Affinity measurements were performed using a human pMHC class I allele, HLA-A2, with mutations in the α3 domain that abolish CD8 cooperation in TCR-pMHC binding (hereafter referred to as HLA-A2-CD8mut) similar to a previous study (*11*). Nonspecific binding with primary $CD8^+$ T cells was negligible within a large range of pMHC site densities (fig. S1). Using a panel of $CD8^+$ T cell clones, we confirmed that the adhesion frequency curve fit the model for bimolecular interactions (Fig. 2A, fig. S3, and eq. S1) (*15*) and the use of wild-type streptavidin as a means to present pMHC on RBC membrane did not cause alterations of 2D affinity via possible multivalent interactions (fig. S2) (*5*).

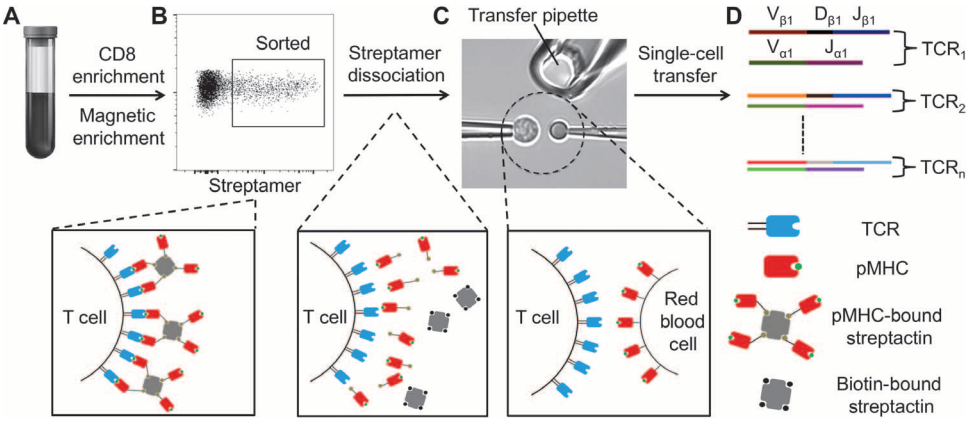

Fig. 1. Overview of the iTAST method. (**A** and **B**) A human blood sample is enriched for $CD8^+$ $streptamer^+$ T cells (A), is sorted using flow cytometry (B), and then undergoes streptamer dissociation by addition of excess biotin. (**C** and **D**) T cells are affinity-tested using a micropipette adhesion assay (C) and then picked for paired single-cell TCR sequencing (D).

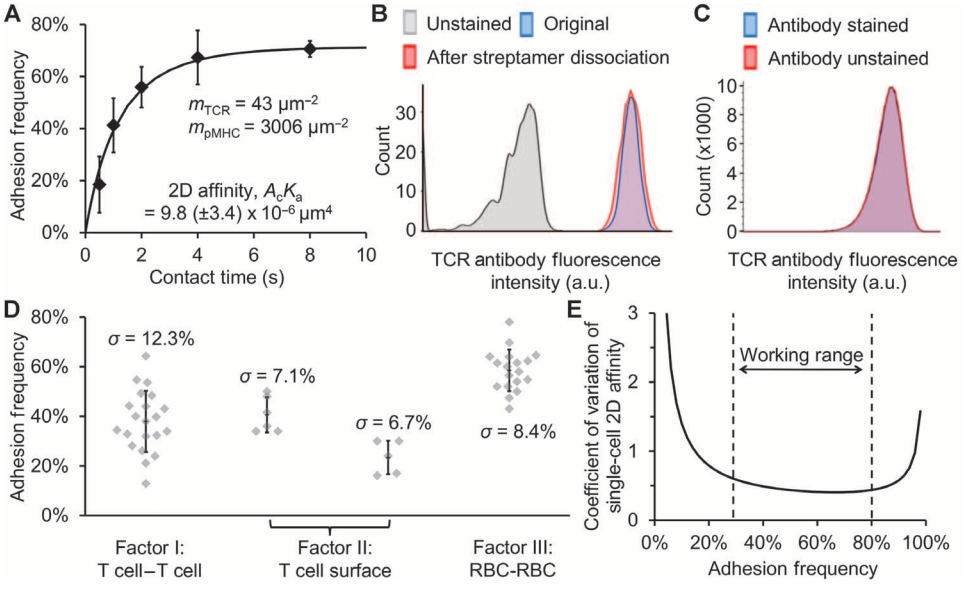

Fig. 2. Verification of single-cell 2D affinity measurement by iTAST. (**A**) Adhesion curve for an HCV-specific $CD8^+$ T cell clone against HLA-A2-CD8mut/HCV. (**B**) TCR expression of an HCV-specific $CD8^+$ T cell and its expression after streptamer staining and dissociation. a.u., arbitrary units. (**C**) TCR expression of $CD8^+$ T cells that were stained with phenotypic antibodies (CD27, CD45RA, CD57, CXCR3, CD95, CD45RO, and CCR7) for 3 hours at room temperature to mimic the environment for single-cell 2D affinity measurement. (**D**) Error analysis of factors associated with single-cell 2D affinity measurement. Factor I: T cell to T cell variation of TCR site density assessed by using one TCR antibody–conjugated RBC against multiple primary $CD8^+$ T cells (each point indicates one T cell). Factor II: Variation of TCR site density in different areas on the same T cell assessed by using one TCR antibody–conjugated RBC against different areas of one T cell (each point indicates one area of the same T cell) (two T cells tested). Although the absolute adhesion frequencies are different between these two T cells, the variations of different areas of one T cell are similar between these two T cells. Factor III: RBC to RBC variation of MHC site density assessed by using one HCV-specific $CD8^+$ T cell clone against multiple HLA-A2-CD8mut/HCV–coated RBCs (each point indicates one RBC). (**E**) Simulation of coefficient of variation at different adhesion frequency values using values measured from (D) and eq. S2.

Single-cell 2D affinity measured in iTAST is a function of the adhesion frequency at a saturating contact time, as well as the TCR and pMHC site density (number of TCR or pMHC molecules per square micrometer area) measured using respective antibodies (Eq. 1) (*5*). Using $CD8^+$ T cell clones, we found that 4 s was sufficient to achieve saturating adhesion frequency for a large range of TCR-pMHC affinities (Fig. 2A and fig. S3). Since TCR site density cannot be directly measured on single $streptamer^+$ $CD8^+$ T cells because TCR antibodies would interfere with pMHC binding, we inferred it by measuring TCR site density from bulk $CD8^+$ T cells from the same donor. We verified that $streptamer^+$ $CD8^+$ T cells had the same TCR site density as bulk $CD8^+$ T cells because streptamers completely dissociated from the cell surface (fig. S4A) and did not alter TCR expression (Fig. 2B). In addition, the ligation of common phenotypic antibodies did not change the TCR expression during affinity measurement (Fig. 2C), and streptamers also performed similarly to conventional streptavidin-based tetramers in staining intensity (fig. S4B).

Error analysis on single-cell 2D affinity measured by iTAST

Single-cell 2D affinity measurement is subject to multiple variables that affect precision, which requires a systematic understanding of the sources of error to develop a stringent validation process. Further, this ensures that the measured TCR affinities and sequences are trustworthy in downstream applications, such as ACT. To estimate this error, we isolated and measured the variance of all factors associated with the single-cell 2D affinity measurement by iTAST (Fig. 2D and fig. S5). This includes variations in (i) TCR site density between T cells, (ii) TCR site density spatial homogeneity within one cell, and (iii) variations in pMHC site density between

RBCs (Fig. 2D). TCR site density variation between T cells contributed the most, at ~70% of the total variance (fig. S5). By integrating these variances, we found that by keeping the adhesion frequency between 30 and 80%, the coefficient of variation of single-cell 2D affinity can be kept below 50% (Fig. 2E).

Comparing single-cell 2D affinity with conventional 2D affinity

The conventional 2D affinity assay cannot be used to study the affinity of single primary antigen-specific T cells in a polyclonal population because it relies on averaging several measurements from a population of clonally identical T cells. In contrast, iTAST can obtain affinities from single cells and provide an estimated variance. To empirically determine the accuracy of single-cell 2D affinity to conventional 2D affinity, we in vitro expanded HCV-specific $CD8^+$ T cell clones and measured their single-cell and conventional 2D affinity using one cell or four to five cells, respectively (Fig. 3A). A significant log-log linear correlation with low variance on the residuals was observed, indicating high accuracy between single-cell and conventional measurements ($P < 10^{-4}$). Next, we verified the accuracy of single-cell 2D affinity directly on primary cells by affinity testing a primary $CD8^+$ T cell and then transferring it for in vitro expansion into a clonal population (Fig. 3B). We found that the single-cell 2D affinity of the primary T cell was similar to the conventional 2D affinity of its resulting clone. The estimated variance in the single-cell 2D affinity was also within 1 SD of the resulting T cell clone, indicating the accuracy of our variance estimate (Fig. 2E and table S1). These results show that single-cell 2D affinity measured by iTAST is a reliable surrogate for conventional 2D affinity with comparable levels of variance (Fig. 3, A and B).

Comparing single-cell 2D affinity measured by iTAST with affinity by SPR

We also validated the consistency of single-cell 2D affinity by iTAST with the gold standard SPR measurement. We used the 1G4 TCR that binds to the human tumor antigen NY-ESO-1 as a model system (*17*). Using the native and peptide variants of NY-ESO-1, we found a significant correlation between single-cell 2D affinities and previously published 3D affinities in the 1G4 system ($P < 0.01$; Fig. 3C and table S2) (*3*). Thus, single-cell 2D affinity could accurately discriminate pMHC ligands with different affinities despite the variance associated with single-cell measurement.

iTAST affinity correlation with functional status

Given the potential of iTAST in immune monitoring and ACT immunotherapy, we next investigated the relationship between single-cell 2D affinity and cell function. Forty-three single HCV-specific $CD8^+$ T cells from HCV-seronegative donors were isolated using HLA-A2/HCV tetramers and in vitro expanded into clones for functionality testing. Although all clones bound specifically in the 2D affinity measurement, not all clones were functional (Fig. 4A). We found that single-cell 2D affinity correlated significantly with lysis capacity and provided a sharp threshold for functionality at a 2D affinity of ~2×10^5 μm^4 ($P < 10^{-4}$).

In addition to functional status, TCR-pMHC affinity also affects the peptide potency, which we define as the minimum peptide concentration required for $CD8^+$ T cells to induce 10% specific lysis of JY cells pulsed with HCV peptide. Peptide potency is a critical parameter for the in vivo efficacy of $CD8^+$ T cells because it is related to the minimum antigenic load required to activate the T cell and elicit a functional response. From HCV-specific $CD8^+$ T cell clones, we found a significant correlation between single-cell 2D affinity and peptide potency ($P < 0.005$; Fig. 4B and fig. S6). A competing and widely used in situ technique to identify highly potent $CD8^+$ T cells is by staining intensity with HLA-A2-CD8mut tetramers (*18*). We did not observe a correlation in tetramer staining with either lysis capacity or peptide potency (Fig. 4, C and D). Although all clones that stained tetramer above background levels were functional, in agreement with past studies (*18*), multiple clones did not stain despite having a lysis capacity and potency comparable to positively stained cells. This high false-negative rate was not seen with single-cell 2D affinities and thus offers higher predictive value than tetramer staining. In addition, all correlations made using single-cell 2D affinity were consistent with conventional 2D affinity made by averaging several measurements in each of the T cell clones (fig. S7).

Affinity repertoire of naïve virus-specific $CD8^+$ T cells and association with age

We applied iTAST to study the affinity distribution of antigen-specific $CD8^+$ T cell precursors in healthy individuals who have not been exposed to their cognate antigen. Antigen-specific T cells are a heterogeneous population that recognize the same pMHC using different TCRs generated by V(D)J recombination (*16*). In unexposed individuals, these cells are extremely rare and exist at a frequency of 1 in 10^4 to 10^6 $CD8^+$ T cells (*16*). As a model system, we isolated the naïve HCV-specific $CD8^+$ T cell population within healthy HCV-seronegative blood donors that binds the HCVns3:1406-1415 (KLVALGINAV) epitope complexed with HLA-A2 (*16*).

HCV-specific $CD8^+$ T cells isolated from 12 samples, derived from nine unique donors, were found to have frequencies ranging from 2 to 18 in 10^6 total $CD8^+$ T cells (fig. S8), consistent with a previous study (*16*). From one unit of leukapheresis, we obtained between 50 and 1000 HCV-specific T cells. We found a surprisingly

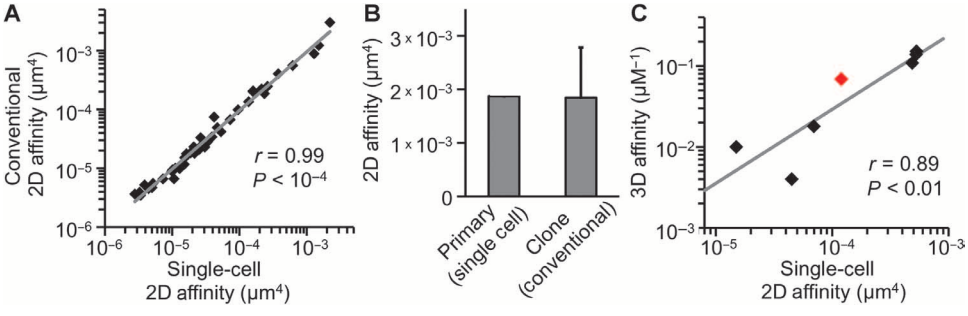

Fig. 3. Comparison of single-cell 2D affinity by iTAST with conventional 2D affinity and SPR. (**A**) Correlation of single-cell 2D affinity and conventional 2D affinity from HCV-specific $CD8^+$ T cell clones ($n = 43$; line denotes log-log linear regression; two-tailed t test on the slope, $P < 10^{-4}$). (**B**) 2D affinity for a primary $CD8^+$ T cell and its clone after being picked into culture well for in vitro expansion. Tabular data available in table S1. (**C**) Correlation of single-cell 2D affinity of the native NY-ESO-1:157-165, denoted in red, and six peptide variants on HLA-A2-CD8mut against the 1G4 TCR expressed on the Jurkat cell line versus 3D affinity by a previously published SPR study (*3*) ($n = 7$; line denotes log-log linear regression; two-tailed t test on the slope, $P < 0.01$). Tabular data available in table S2.

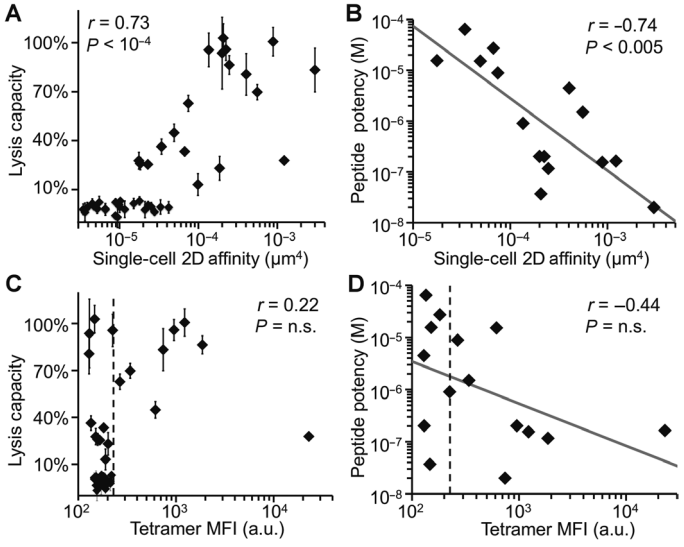

Fig. 4. Correlation of single-cell 2D affinity with functional capacity. (**A**) Single-cell 2D affinity of HCV-specific CD8$^+$ T cells versus their lysis capacity, defined as the percent specific lysis of HCV peptide-pulsed JY cells (n = 43; Spearman two-tailed test, $P < 10^{-4}$). (**B**) Single-cell 2D affinity versus peptide potency, defined as the peptide concentration required to induce 10% cell lysis (n = 15; line denotes log-log linear regression; two-tailed t test on the slope, $P < 0.005$). (**C** and **D**) HLA-A2-CD8mut/HCV tetramer median fluorescence intensity (MFI) versus (C) lysis capacity (Spearman two-tailed test) and (D) peptide potency (log-log linear regression, two-tailed t test on the slope). Dashed line denotes limit of detection in tetramer staining. n.s., not significant.

large affinity range of more than 1000-fold within this antigen-specific T cell repertoire (Fig. 5A). We observed consistent heterogeneity in the affinity distributions of HCV-specific CD8$^+$ T cell populations between the donors (Fig. 5A). Samples 4A and 4B and samples 5A, 5B, and 5C represent repeated blood draws from donors 4 and 5, respectively, collected within a 7-month time span. Samples from the same donor exhibited similar distributions in T cell affinity, whereas the distributions between donors 4 and 5 were significantly different, with the latter containing a lower median T cell affinity ($P < 0.005$). We also translated 2D affinities into the number of pMHCs required to form, on average, one bond with TCR at 4 s of contact (Eq. 2 and Fig. 5B); we note that this value would be an overestimation of the actual number of pMHCs required because it does not take into account possible transient binding at earlier times. Given this, the 2D affinity range translates to a requirement of at most ~5 pMHCs to bind a T cell with the highest-affinity and ~50,000 pMHCs for the lowest-affinity T cell (Fig. 5B).

To investigate whether this heterogeneity is associated with age, we recruited additional healthy HCV-seronegative donors 33 or younger and 49 or older for iTAST measurement. From nine unique donors, we found that the naïve HCV-specific CD8$^+$ T cell repertoire within young donors had a significantly higher median 2D affinity than older donors ($P < 0.05$; Fig. 5C). From the 2D affinity threshold of 2×10^{-5} μm^4 previously determined for in vitro functionality (Fig. 4A), we also found that older donors contain a significantly lower fraction of functionally competent HCV-specific CD8$^+$ T cells than younger donors ($P < 0.005$; fig. S9 and table S3).

Association of TCR affinity and sequence

Affinity-tested T cells from samples 4B, 5A, 6, and 7 were picked for single-cell TCR amplification and sequencing. A success rate of 43 to 56% for TCRα and 44 to 75% for TCRβ was achieved, which is comparable to other single-cell TCR amplification methods (*13*), and no RNA contamination was found between consecutive T cell transfers (fig. S10). We found a surprisingly narrow TCRα V-gene (TRAV) usage composed almost exclusively of TRAV38-2, whereas TCRβ V-gene (TRBV) usage was more diverse (Fig. 5D); this trend was consistent among all four donors (fig. S11). TCRs bearing TRAV38-2 recapitulated the entire affinity range and did not differ in 2D affinity from TCRs without TRAV38-2 (table S4).

In addition, we observed two pairs of T cells, each bearing an identical TCRα amino acid sequence but different TCRβ sequences that were isolated from separate donors (table S4, red). The first TCR pair also shared the same TRBV, with differences only in the CDR3β region. Despite this similarity, their 2D affinity differed by 50-fold (2.2×10^{-4} versus 4.2×10^{-6} μm^4). The higher-affinity TCR contained a greater proportion of hydrophobic residues in the CDR3β region (CASKMGAEAFF, 54% hydrophobic) than the lower-affinity TCR (CASGQGQETQYF, 17% hydrophobic). It is likely that hydrophobic residues in the CDR3β region interact with the largely hydrophobic HCV peptide (KLVALGINAV, 70% hydrophobic) to increase TCR affinity. This observation is supported by the second TCR pair, where a smaller 2D affinity difference of 2.5-fold (1.1×10^{-5} μm^4 versus 4.4×10^{-6} μm^4) was associated with a smaller difference in the proportion of CDRβ hydrophobic residues between the high-affinity (CASSLEREGRGEQFF, 27% hydrophobic) and low-affinity (CATSIDRGREKLFF, 36% hydrophobic) TCRs. Thus, hydrophobic residues in the CDR3β chain are potential regulators of TCR affinity with the HCV peptide.

DISCUSSION

Continued interest in TCR-pMHC affinity stems from the observation that TCR-pMHC binding parameters influence the subsequent downstream T cell response. Here, we present a high-throughput strategy for measuring TCR affinity and its corresponding TCR sequence, enabling direct measurement of primary CD8$^+$ T cells from human blood of any specificity. Using the 1G4 TCR, we found that single-cell 2D affinity obtained by iTAST correlates with the widely used 3D affinity by SPR. The variance associated with single-cell measurement was low compared to the 1000-fold range of 2D affinity associated with primary CD8$^+$ T cells, allowing accurate discrimination of high- and low-affinity TCRs. This makes single-cell 2D affinity a reliable surrogate for 3D affinity by SPR that is quicker to obtain and does not require soluble TCR production.

This correlation also shows the applicability of iTAST to ACT because affinity measured by SPR is widely believed to correlate with the efficacy of ACT in cancer (*19*). A variant of the 1G4 TCR used in our study with high affinity by SPR was recently used for ACT with successful therapeutic responses in patients with multiple myeloma (*20*). For ACT in cancer, current approaches using directed evolution to increase TCR affinity can cause reduced specificity and create fatal cross-reactivity (*6*). With iTAST, the ability to isolate TCRs native to humans with a given affinity could enable rapid selection of safer candidate TCRs with high potency.

Single-cell 2D affinity by iTAST also correlated with both T cell functional status and potency from a panel of HCV-specific CD8$^+$ T cell clones. Despite specific binding to pMHC ligand, not all clones were capable of lysing target cells. Single-cell 2D affinity was able to define a sharp threshold between the functional and nonfunctional T cells, whereas tetramer staining could not. A large fraction of primary

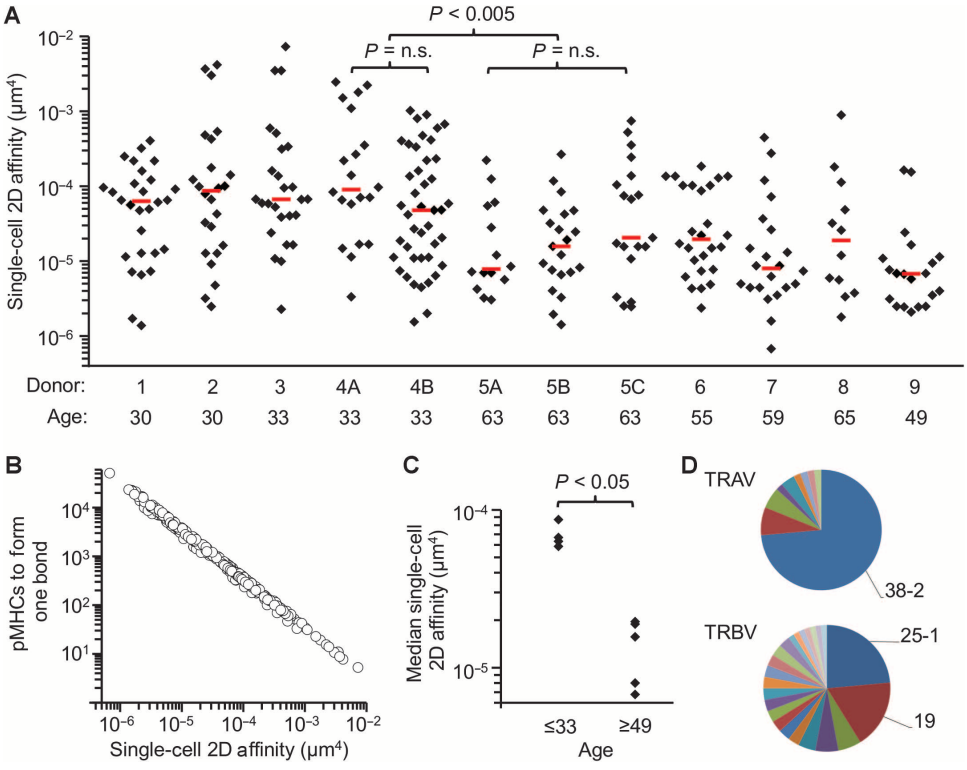

Fig. 5. Analysis of the primary HCV-specific CD8⁺ T cell repertoire in HCV-seronegative blood donors using iTAST. (**A**) Single-cell 2D affinity distribution of naïve primary HCV-specific CD8⁺ T cells within 12 HCV-seronegative samples from nine donors. Numbers indicate different donors, and letters indicate separate blood draws from the same donor. Red bar indicates median value. 2D affinities transformed by $\log_{10}$ for *t* test in 4A and 4B ($n = 63$), analysis of variance (ANOVA) in 5A, 5B, and 5C ($n = 54$), and *t* test in aggregate 2D affinities from donors 4 and 5 ($n = 117$, $P < 0.005$). Two-tailed test is used in all cases. (**B**) Relation of single-cell 2D affinity with the number of pMHCs required to form one TCR-pMHC bond at 4 s of contact. (**C**) Median single-cell 2D affinity for each unique donor from (A). Samples derived from the same donor were aggregated before calculation ($n = 9$; two-tailed Mann-Whitney *U* test, $P < 0.05$). Tabular data available in table S3. (**D**) TRAV and TRBV usage of T cells from samples 4B, 5A, 6, and 7 in (A).

HCV-specific CD8⁺ T cells were below this affinity threshold, indicating that they may not have protective capacity. This value corresponds to an upper limit of ~1200 pMHCs for TCR-pMHC bond formation at 4 s of contact, which is in agreement with the upper bound of ~400 pMHCs required for T cell functionality in literature (*21*). Because both the T cell clones and primary T cells were isolated using tetramers, solely using tetramer staining can potentially overestimate the antigen-specific CD8⁺ T cell frequency because not all cells have functional potential.

We also characterized the TCR affinity range associated with naïve HCV-specific CD8⁺ T cell populations in unexposed human individuals. Naïve T cells are believed to be the safety net against infection and cancer and are the targets of vaccination (*16*). In addition, naïve virus-specific CD8⁺ T cell populations have recently been shown to be a potential source for ACT against persistent viral infections, which makes hunting for high-affinity primary T cells a high priority (*8*). The 1000-fold range of TCR affinity found here demonstrates the superb sensitivity and large dynamic range (*21*) that T cells have to antigens. Especially among young donors, many T cells contain TCRs with 2D affinities that are comparable or even higher than the OT1 TCR against the ovalbumin peptide (2.4×10^{-4} μm⁴), a well-known high-affinity TCR-pMHC interaction (*5*). Past studies have observed a ~100-fold range based on aggregate SPR affinity measurements using multiple MHC alleles, epitopes, and donor sources (*22*). Here, we show that such a large dynamic range exists even within the antigen-specific T cell population for a single pMHC epitope within a single donor. At the same time, it represents a challenge of how to accurately select a TCR with optimum affinity for ACT. Our study illustrates the usefulness of iTAST as a quick method to directly evaluate the quality of this immune safety net and accurately pinpoint TCRs with a particular affinity and sequence for ACT and other immune engineering applications.

The observation that the TCR affinity distribution is similar within separate blood draws from the same donor indicates the reproducibility of iTAST. The difference observed in affinity distributions between donors shows that alterations in this parameter can be detected by iTAST and highlights its usefulness as a reliable and unique signature for immune monitoring applications.

We further determined that this change in affinity distribution is associated with age. It is well known that aging reduces the TCR diversity and size through reduced thymic output and increased homeostatic proliferation (*23*). Recent studies in mice have demonstrated that attrition of the precursor foreign-specific T cell population with age is nonrandom due to preferential use of particular TCR V-genes (*24*). Here, we demonstrate that changes in the T cell affinity repertoire are also nonrandom, because older donors contained a significantly lower proportion of high-affinity HCV-specific CD8⁺ T cells than young donors ($P < 0.005$; fig. S9). This reduced frequency of high-affinity virus-specific T cells could be a contributing factor toward the increased risk of infection and diminished vaccine response in the elderly. In particular, decreases in T cell affinity could be a mechanism for the creation of holes in the T cell repertoire, as observed in the reduced T cell response with age in a mouse influenza virus model (*25*). Lastly, this result also suggests that young donors are a better source of high-affinity TCRs for adoptive transfer applications than older donors.

The ability to obtain correlated TCR sequence and affinity from these donors provides an additional dimension for antigen-specific T cell analysis. The dominance of the TRAV38-2 gene among all donors compared to the larger diversity of TRBVs suggests that the TRAV38-2 V-gene has an intrinsic affinity to the HLA-A2/HCV epitope. However, TCRs bearing TRAV38-2 spanned the entire dynamic range of TCR affinity, suggesting that additional factors are required for binding. One such factor we observed involved the use of hydrophobic residues in the CDR3β to interact with the largely hydrophobic HCV peptide. It is possible that whereas the TCRα chain imparts specificity to HLA-A2/HCV, the TCRβ CDR3 can regulate the affinity of the interaction. This is also

consistent with the large diversity of TRBV usage compared to TCRα, and is in line with recent evidence that whereas one TCR chain can dictate specificity, the other TCR chain can regulate the functionality over a broad range (*26*).

We note several limitations to the current study that warrants further development. It is unknown whether the decrease in TCR affinity with age is a general trend associated with foreign-specific $CD8^+$ T cell populations or whether it is an epitope-specific phenomenon. In addition, although the current throughput of iTAST enables it to address many important biological questions, it will be useful to further automate this system and increase throughput.

Here, we present a method for rapid in situ measurement of TCR-pMHC affinity and sequence directly from primary $CD8^+$ T cells isolated from human blood. The low–cell count requirement allows iTAST to be applied to wide-ranging human sample types, from peripheral blood to primary tumors. iTAST offers a quick, reliable, and unbiased way to identify candidate TCRs with high affinity and high potency for immunotherapy. In addition, the ability to obtain TCR-pMHC affinity distribution from primary T cells allows iTAST to address questions of how the T cell repertoire changes due to age, autoimmune disease, viral infection, and cancer. Overall, we believe that iTAST will find broad applications in basic research into TCR affinity as well as clinical applications in immune profiling and adoptive immunotherapy.

MATERIALS AND METHODS

Study design

The objective of this study was to characterize the TCR sequence and affinity distribution of precursor antigen-specific $CD8^+$ T cells within healthy human individuals of different ages using iTAST. Donors were assigned unique serial numbers to identify repeat donors. Researchers had access only to donor age, gender, cytomegalovirus (CMV) serostatus, and infectious disease status (including HCV). This study was not blinded, and sample selection was not random. Samples were CMV-seronegative males and selected on the basis of the age criteria of less than or equal to 33 years and greater than or equal to 49 years.

The authors initially determined affinity distributions from samples 4B, 5A, 5B, and 9 and observed a dependence on the T cell affinity distribution with age. We measured the affinity distribution of six additional unique donors and used the ratio of T cells with high affinity ($\geq 2 \times 10^{-5}$ μm^4) and low affinity ($<2 \times 10^{-5}$ μm^4) from each donor as a metric. On the basis of this metric and the preliminary results, we found that a total of nine donors would be sufficient to differentiate the two age groups with 90% power in a two-tailed *t* test with $P = 0.05$. In addition, two biological replicates of primary T cell affinity by iTAST were performed for donor 4; blood draws were made within a 7-month time span. Three biological replicates were performed for donor 5; blood draws were made within a 3-month time span.

Streptamer sorting and dissociation

Human leukocyte reduction system chambers were obtained from deidentified donors at the Blood and Tissue Center of Central Texas with strict adherence to guidelines from the Institutional Review Board (study number 2013-09-0041) of the University of Texas at Austin. $CD8^+$ T cell enrichment was done following the protocol described previously (*16*, *27*) using RosetteSep $CD8^+$ T Cell Enrichment Cocktail (STEMCELL) together with Ficoll-Paque (GE Healthcare). Then, RBCs were lysed using ACK Lysing Buffer (Lonza). After washing in phosphate-buffered saline with fetal bovine serum, the cell mixture was passed through a cell strainer (Corning) and ready for use. For the remainder of the experiment, the cells were kept either on ice or at 4°C in refrigerator.

The entire procedure was performed either on ice or at 4°C following a published protocol (*16*, *27*) using streptamer instead of regular tetramer with Miltenyi anti-phycoerythrin (PE) microbeads and column. Sodium azide was added to cell buffer. The flow-through was collected for background staining and frequency calculation. The enriched fraction was eluted off the column and washed into cell buffer. The following antibody panel was used to stain both the enriched and flow-through fractions: CD4, CD14, CD16, CD19, CD32, and CD56 (BioLegend) as a dump channel to stain residual non-$CD8^+$ T cells, and CD45RA, CCR7, and CD27 (BioLegend). 7-Aminoactinomycin D was used as a viability marker.

The antibody-stained enriched fraction was washed, and counting beads were added. Naïve streptamer-positive $CD8^+$ T cells were sorted using BD FACSAria II system into cell buffer as described previously with minor modifications (*14*). After dissociation, cells were washed twice in medium and stored at 4°C until the iTAST experiment.

Measuring primary single-cell 2D affinity and transfer for sequencing

Streptamer-dissociated antigen-specific T cells were added to the microscope chamber, along with five populations of RBCs carrying HLA-A2-CD8mut/HCV with different site densities. RBC site densities ranged from ~5 to ~2000 sites/μm^2. Derived from eq. S1, as contact time goes to infinity, adhesion frequency reaches an equilibrium value:

$$A_c K_a = \frac{-\ln(1 - P_{a,eq})}{m_r m_l} \quad (1)$$

where $P_{a,eq}$ is the equilibrium adhesion frequency, m_r is the TCR site density, m_l is the pMHC site density, A_c is the contact area, and $A_c K_a$ is the 2D affinity. For primary T cell affinities, we determined the single-cell 2D affinity value using Eq. 1 and by measuring the adhesion frequency at 4 s. If the adhesion frequency is lower than 30% or higher than 80% after 10 contacts, then a new RBC with a higher or lower site density, respectively, is used, and adhesion frequency is measured again until 30 to 80% is reached for 10 contacts. Twenty-five contacts were measured for each T cell–RBC pair. The test chamber was engineered to facilitate the transferring of cells out of the chamber to PCR tubes using a third pipette.

Another way to use the adhesion frequency P_a is for calculating the average number of bonds, $<n>$ (*11*):

$$P_a = 1 - e^{-<n>}$$

$$<n> = m_r m_l A_c K_a$$

We can then derive the number of pMHCs required for an average bond number of 1 to form, using 3 μm^2 to approximate the contact area, which was also kept constant throughout experiments:

$$\text{Number of pMHC to form one bond} = \frac{A_c m_l}{<n>} = -\frac{A_c m_l}{\ln(1 - P_a)} \quad (2)$$

It should be noted that this value does not take into account bonds that were dissociated before 4 s nor does it take into account the lifetime

of a bond, and so, our calculation would be an overestimation of the actual required number of pMHCs.

HCV-specific CD8$^+$ T cell lines

HCV-specific CD8$^+$ T cell lines were generated according to a previously published protocol (*16*). Conventional streptavidin-based tetramers were used to sort single cells into medium using the same isolation procedure as streptamer. Functional status was analyzed 10 to 21 days after restimulation.

Tetramer preparation and staining of CD8$^+$ T cell clones

Ultraviolet (UV)–exchanged tetramer was prepared as previously described (*16*, *28*). HLA-A2-CD8mut was obtained from the National Institutes of Health Tetramer Core Facility. PE-labeled streptavidin was from BioLegend.

For tetramer staining, HCV-specific CD8$^+$ T cell clones were incubated with 0.14 μg of HLA-A2-CD8mut/HCV and 2 μl of CD8 blocking antibody (EMD Millipore, clone DK25) in 50 μl of cell buffer for 1 hour at 4°C. Cells were washed using cell buffer and then analyzed using BD Fortessa.

Statistical analysis

Statistical tests used are detailed in the figure legends. Shapiro-Wilk and Brown-Forsythe tests were performed to ensure that the data are normally distributed and with equal variance, respectively, for either two-sample *t* test or ANOVA for multiple sample comparison. The α value for statistical significance was 0.05 unless otherwise stated; Bonferroni correction to $\alpha = 0.017$ was used in Fig. 5A. Equal variances were checked by Brown-Forsythe in Mann-Whitney *U* test. The authors consulted with the University of Texas at Austin Department of Statistics and Data Sciences. The JMP software was used for all statistical analyses.

SUPPLEMENTARY MATERIALS

www.sciencetranslationalmedicine.org/cgi/content/full/8/341/341ra77/DC1
Materials and Methods
Fig. S1. Nonspecific adhesion on primary CD8$^+$ T cells is negligible and not correlated with pMHC site density.
Fig. S2. Multivalency of pMHC does not affect 2D affinity measurement.
Fig. S3. 2D affinity kinetic curves for three additional CD8$^+$ T cell clones with varying affinities.
Fig. S4. Streptamer staining is fully reversible, and streptamers stain with the same intensity as conventional tetramers.
Fig. S5. Estimating the error of single-cell 2D affinity measurements.
Fig. S6. Peptide titration curves of 15 HCV-specific CD8$^+$ T cell clones.
Fig. S7. Conventional 2D affinity measurement on HCV-specific CD8$^+$ T cell clones shows similar correlations as single-cell 2D affinity.
Fig. S8. Gating strategy for sorting HCV-streptamer$^+$ T cells.
Fig. S9. Ratio of high-affinity/low-affinity HCV-specific CD8$^+$ T cells based on functional potential.
Fig. S10. Amplification efficiency of affinity-tested cells.
Fig. S11. TRAV and TRBV usage of affinity-tested primary HCV-specific CD8$^+$ T cells by donor.
Table S1. Comparison of single-cell 2D affinity derived from a primary T cell and conventional 2D affinity derived from the T cell's in vitro expanded clone.
Table S2. Single-cell 2D affinity and SPR 3D affinity for the native and peptide variants of NY-ESO-1 against 1G4 TCR.
Table S3. Median 2D affinity and ratio of high/low 2D affinity from primary HCV-specific CD8$^+$ T cells.
Table S4. Single-cell 2D affinity and correlated TCRα and TCRβ CDR3 sequences.
Reference (*29*)

REFERENCES AND NOTES

1. M. Krogsgaard, M. M. Davis, How T cells 'see' antigen. *Nat. Immunol.* **6**, 239–245 (2005).
2. C. G. King, S. Koehli, B. Hausmann, M. Schmaler, D. Zehn, E. Palmer, T cell affinity regulates asymmetric division, effector cell differentiation, and tissue pathology. *Immunity* **37**, 709–720 (2012).
3. M. Aleksic, O. Dushek, H. Zhang, E. Shenderov, J.-L. Chen, V. Cerundolo, D. Coombs, P. A. van der Merwe, Dependence of T cell antigen recognition on T cell receptor-peptide MHC confinement time. *Immunity* **32**, 163–174 (2010).
4. J.-L. Chen, A. J. Morgan, G. Stewart-Jones, D. Shepherd, G. Bossi, L. Wooldridge, S. L. Hutchinson, A. K. Sewell, G. M. Griffiths, P. A. van der Merwe, E. Y. Jones, A. Galione, V. Cerundolo, Ca^{2+} release from the endoplasmic reticulum of NY-ESO-1–specific T cells is modulated by the affinity of TCR and by the use of the CD8 coreceptor. *J. Immunol.* **184**, 1829–1839 (2010).
5. J. Huang, V. I. Zarnitsyna, B. Liu, L. J. Edwards, N. Jiang, B. D. Evavold, C. Zhu, The kinetics of two-dimensional TCR and pMHC interactions determine T-cell responsiveness. *Nature* **464**, 932–936 (2010).
6. N. P. Restifo, M. E. Dudley, S. A. Rosenberg, Adoptive immunotherapy for cancer: Harnessing the T cell response. *Nat. Rev. Immunol.* **12**, 269–281 (2012).
7. M. Nauerth, B. Weißbrich, R. Knall, T. Franz, G. Dössinger, J. Bet, P. J. Paszkiewicz, L. Pfeifer, M. Bunse, W. Uckert, R. Holtappels, D. Gillert-Marien, M. Neuenhahn, A. Krackhardt, M. J. Reddehase, S. R. Riddell, D. H. Busch, TCR-ligand k_{off} rate correlates with the protective capacity of antigen-specific CD8$^+$ T cells for adoptive transfer. *Sci. Transl. Med.* **5**, 192ra87 (2013).
8. P. J. Hanley, J. J. Melenhorst, S. Nikiforow, P. Scheinberg, J. W. Blaney, G. Demmler-Harrison, C. R. Cruz, S. Lam, R. A. Krance, K. S. Leung, C. A. Martinez, H. Liu, D. C. Douek, H. E. Heslop, C. M. Rooney, E. J. Shpall, A. J. Barrett, J. R. Rodgers, C. M. Bollard, CMV-specific T cells generated from naïve T cells recognize atypical epitopes and may be protective in vivo. *Sci. Transl. Med.* **7**, 285ra63 (2015).
9. J. B. Huppa, M. Axmann, M. A. Mortelmaier, B. F. Lillemeier, E. W. Newell, M. Brameshuber, L. O. Klein, G. J. Schütz, M. M. Davis, TCR–peptide–MHC interactions in situ show accelerated kinetics and increased affinity. *Nature* **463**, 963–967 (2010).
10. E. L. Frost, A. E. Kersh, B. D. Evavold, A. E. Lukacher, Cutting edge: Resident memory CD8 T cells express high-affinity TCRs. *J. Immunol.* **195**, 3520–3524 (2015).
11. N. Jiang, J. Huang, L. J. Edwards, B. Liu, Y. Zhang, C. D. Beal, B. D. Evavold, C. Zhu, Two-stage cooperative T cell receptor-peptide major histocompatibility complex-CD8 trimolecular interactions amplify antigen discrimination. *Immunity* **34**, 13–23 (2011).
12. D. Zehn, S. Y. Lee, M. J. Bevan, Complete but curtailed T-cell response to very low-affinity antigen. *Nature* **458**, 211–214 (2009).
13. A. Han, J. Glanville, L. Hansmann, M. M. Davis, Linking T-cell receptor sequence to functional phenotype at the single-cell level. *Nat. Biotechnol.* **32**, 684–692 (2014).
14. M. Knabel, T. J. Franz, M. Schiemann, A. Wulf, B. Villmow, B. Schmidt, H. Bernhard, H. Wagner, D. H. Busch, Reversible MHC multimer staining for functional isolation of T-cell populations and effective adoptive transfer. *Nat. Med.* **8**, 631–637 (2002).
15. S. E. Chesla, P. Selvaraj, C. Zhu, Measuring two-dimensional receptor-ligand binding kinetics by micropipette. *Biophys. J.* **75**, 1553–1572 (1998).
16. W. Yu, N. Jiang, P. J. R. Ebert, B. A. Kidd, S. Müller, P. J. Lund, J. Juang, K. Adachi, T. Tse, M. E. Birnbaum, E. W. Newell, D. M. Wilson, G. M. Grotenbreg, S. Valitutti, S. R. Quake, M. M. Davis, Clonal deletion prunes but does not eliminate self-specific αβ CD8$^+$ T lymphocytes. *Immunity* **42**, 929–941 (2015).
17. J.-L. Chen, G. Stewart-Jones, G. Bossi, N. M. Lissin, L. Wooldridge, E. M. L. Choi, G. Held, P. R. Dunbar, R. M. Esnouf, M. Sami, J. M. Boulter, P. Rizkallah, C. Renner, A. Sewell, P. A. van der Merwe, B. K. Jakobsen, G. Griffiths, E. Y. Jones, V. Cerundolo, Structural and kinetic basis for heightened immunogenicity of T cell vaccines. *J. Exp. Med.* **201**, 1243–1255 (2005).
18. M. Bodinier, M.-A. Peyrat, C. Tournay, F. Davodeau, F. Romagne, M. Bonneville, F. Lang, Efficient detection and immunomagnetic sorting of specific T cells using multimers of MHC class I and peptide with reduced CD8 binding. *Nat. Med.* **6**, 707–710 (2000).
19. S. Zhong, K. Malecek, L. A. Johnson, Z. Yu, E. Vega-Saenz de Miera, F. Darvishian, K. McGary, K. Huang, J. Boyer, E. Corse, Y. Shao, S. A. Rosenberg, N. P. Restifo, I. Osman, M. Krogsgaard, T-cell receptor affinity and avidity defines antitumor response and autoimmunity in T-cell immunotherapy. *Proc. Natl. Acad. Sci. U.S.A.* **110**, 6973–6978 (2013).
20. P. F. Robbins, R. A. Morgan, S. A. Feldman, J. C. Yang, R. M. Sherry, M. E. Dudley, J. R. Wunderlich, A. V. Nahvi, L. J. Helman, C. L. Mackall, U. S. Kammula, M. S. Hughes, N. P. Restifo, M. Raffeld, C.-C. R. Lee, C. L. Levy, Y. F. Li, M. El-Gamil, S. L. Schwarz, C. Laurencot, S. A. Rosenberg, Tumor regression in patients with metastatic synovial cell sarcoma and melanoma using genetically engineered lymphocytes reactive with NY-ESO-1. *J. Clin. Oncol.* **29**, 917–924 (2011).
21. M. M. Davis, M. Krogsgaard, M. Huse, J. Huppa, B. F. Lillemeier, Q.-j. Li, T cells as a self-referential, sensory organ. *Annu. Rev. Immunol.* **25**, 681–695 (2007).
22. J. D. Stone, A. S. Chervin, D. M. Kranz, T-cell receptor binding affinities and kinetics: Impact on T-cell activity and specificity. *Immunology* **126**, 165–176 (2009).
23. J. J. Goronzy, C. M. Weyand, T cell development and receptor diversity during aging. *Curr. Opin. Immunol.* **17**, 468–475 (2005).
24. K. M. Quinn, S. G. Zaloumis, T. Cukalac, W.-T. Kan, X. Y. X. Sng, M. Mirams, K. A. Watson, J. M. McCaw, P. C. Doherty, P. G. Thomas, A. Handel, N. L. La Gruta, Heightened self-reactivity associated with selective survival, but not expansion, of naïve virus-specific CD8$^+$ T cells in aged mice. *Proc. Natl. Acad. Sci. U.S.A.* **113**, 1333–1338 (2016).
25. E. J. Yager, M. Ahmed, K. Lanzer, T. D. Randall, D. L. Woodland, M. A. Blackman, Age-associated decline in T cell repertoire diversity leads to holes in the repertoire and impaired immunity to influenza virus. *J. Exp. Med.* **205**, 711–723 (2008).

26. M. Nakatsugawa, Y. Yamashita, T. Ochi, S. Tanaka, K. Chamoto, T. Guo, M. O. Butler, N. Hirano, Specific roles of each TCR hemichain in generating functional chain-centric TCR. *J. Immunol.* **194**, 3487–3500 (2015).
27. J. J. Moon, H. H. Chu, M. Pepper, S. J. McSorley, S. C. Jameson, R. M. Kedl, M. K. Jenkins, Naive CD4$^+$ T cell frequency varies for different epitopes and predicts repertoire diversity and response magnitude. *Immunity* **27**, 203–213 (2007).
28. M. Toebes, M. Coccoris, A. Bins, B. Rodenko, R. Gomez, N. J. Nieuwkoop, W. van de Kasteele, G. F. Rimmelzwaan, J. B. A. G. Haanen, H. Ovaa, T. N. M. Schumacher, Design and use of conditional MHC class I ligands. *Nat. Med.* **12**, 246–251 (2006).
29. M. Shugay, O. V. Britanova, E. M. Merzlyak, M. A. Turchaninova, I. Z. Mamedov, T. R. Tuganbaev, D. A. Bolotin, D. B. Staroverov, E. V. Putintseva, K. Plevova, C. Linnemann, D. Shagin, S. Pospisilova, S. Lukyanov, T. N. Schumacher, D. M. Chudakov, Towards error-free profiling of immune repertoires. *Nat. Methods* **11**, 653–655 (2014).

Acknowledgments: We thank M. M. Davis, W. Yu, and N. Sigal at the Stanford University for technical insights of antigen-specific T cell enrichment and providing UV-exchangeable tetramer and JY cells; C. Zhu, W. Chen, B. Liu, and A. Ju at the Georgia Institute of Technology for technical insights of micropipette adhesion assay and providing divalent streptavidin; the Genomic Sequencing and Analysis Facility at the University of Texas at Austin for sequencing; the NIH tetramer center for providing CD8 mutant HLA-A2; the Blood and Tissue Center of Central Texas for leukapheresis chambers; V. Cerundolo at the University of Oxford for providing the Jurkat cell line transduced with 1G4 TCR; and E. Cohen for helping with sample coordination. **Funding:** This study was supported by NIH grant R00AG040149 (N.J.), Cancer Prevention and Research Institute of Texas grant R1120 (N.J.), Welch Foundation grant F1785 (N.J.), and Damon Runyon-Rachleff Innovator Award DRR-32-15 (N.J.). S.-Q.Z. is a recipient of Thrust 2000—Archie W. Straiton Endowed Graduate Fellowship in Engineering No. 1, B.S.W. is a recipient of the Thrust 2000—George Sawyer Endowed Graduate Fellowship in Engineering, and A.I.M. is a recipient of the Virginia and Ernest Cockrell Jr. Scholarship in Engineering. **Author contributions:** S.-Q.Z. and N.J. conceived the study; S.-Q.Z. developed the method, performed iTAST experiments, and analyzed the data; S.-Q.Z. and K.-Y.M. performed single-cell TCR sequencing experiment with the help from Q.S. and A.I.M.; C.H. analyzed the sequencing data; P.P., Z.C., and C.M.W. helped with the micropipette experiment on CD8$^+$ T cell clones; B.S.W. helped with flow cytometry; M.A.S. coordinated sample collection; and S.-Q.Z. and N.J. wrote the manuscript with inputs from all authors. **Competing interests:** N.J. is an equity holder of Lineage Biosciences Inc. and was a paid consultant for ImmuMetrix from 2011 to 2014. A provisional patent application (Methods and compositions for detecting single T cell receptor affinity and sequence, application no. 62/320,801) has been filed by the University of Texas at Austin from N.J., S.-Q.Z., K.-Y.M., and C.H. on this method. **Data and materials availability:** All TCR sequences are listed in the Supplementary Materials. Further inquiries should be directed to the corresponding author at jiang@austin.utexas.edu.

Submitted 21 December 2015
Accepted 9 May 2016
Published 1 June 2016
10.1126/scitranslmed.aaf1278

Citation: S.-Q. Zhang, P. Parker, K.-Y. Ma, C. He, Q. Shi, Z. Cui, C. M. Williams, B. S. Wendel, A. I. Meriwether, M. A. Salazar, N. Jiang, Direct measurement of T cell receptor affinity and sequence from naïve antiviral T cells. *Sci. Transl. Med.* **8**, 341ra77 (2016).

Editor's Summary

iTAST: A taste of T cell specificity

There is a well-established link between T cell receptor (TCR) affinity and T cell function, which can have important implications for T cell –based therapies. Zhang *et al.* have now developed a method to concurrently sequence TCRs and measure TCR affinity of individual T cells from humans. Using this technique, they show that older individuals may be less able to respond to viral infections or vaccines due to a lack of high-affinity T cells. This method could help screen T cells for cancer immunotherapy or vaccine responses.